Research Article

Copper distribution and oxidation states near corroded fasteners in treated wood

Samuel L. Zelinka[1] · Joseph E. Jakes[1] · Grant T. Kirker[1] · Leandro Passarini[2] · Christopher G. Hunt[1] · Barry Lai[3] · Olga Antipova[3] · Luxi Li[3] · Stefan Vogt[3]

© This is a U.S. Government work and not under copyright protection in the US; foreign copyright protection may apply 2019

Abstract
Metal fasteners are used to hold wood structures together. In outdoor applications, these fasteners are subject to corrosion when the wood is treated with certain preservative treatments. Typically, these treatments contain copper. Prior work has hypothesized that the mechanism of corrosion in treated wood involves reduction of copper ions from the wood treatments. However, copper was rarely detected in the corrosion products of metals embedded in treated wood, which contradicts the hypothesized mechanism. This present work utilizes synchrotron based X-ray fluorescence microscopy (XFM) and X-ray absorption near edge spectroscopy to examine the corrosion mechanism in treated wood by looking at the spatial distribution and oxidation states of copper in the treated wood near the fastener and in the corrosion products removed from the fastener surface. The samples were obtained after a 1-year corrosion test. In the wood cell walls, the oxidation state of the copper treatment did not change in the immediate vicinity of the fastener, although there was a depletion of copper near the fastener. Furthermore, copper was detected in the corrosion products in trace amounts using XFM. Together, these techniques confirm that the corrosion mechanism involves transport of the cupric ions to the fastener surface, where they are reduced and suggest that previous attempts to detect copper were unsuccessful because the concentration of copper in the corrosion products was below the level of detection of the previously used techniques.

Keywords X-ray fluorescence microscopy (XFM) · X-ray absorption near edge spectroscopy (XANES) · Preservative treated wood · Corrosion · Copper

1 Introduction

Metal fasteners are frequently used to hold wood structures together. While in general wood is not a corrosive material, in certain situations wood can cause corrosion of metal fasteners which can lead to structural failures [1, 2]. Copper based waterborne wood preservatives are frequently used in the United States to protect the wood from fungal and insect attack [3, 4]. These wood preservatives have been shown to increase the corrosion of metal fasteners [5–13].

Corrosion of fasteners in contact with preservative treated wood is believed to involve the reduction of copper ions from the wood preservatives (Fig. 1) [5, 12, 14]. It has been reported that over 95% of the copper from the wood preservative is held within the wood as cupric (Cu^{++}) ions [15]. Thermodynamically, these cupric ions are unstable in the presence of steel or galvanized (zinc coated) steel fasteners in wood as illustrated in Pourbaix diagrams [12]. However, stainless steel fasteners, which are noble to copper in the galvanic series, have negligible corrosion rates in treated and modified wood [11, 16]. Kinetically,

✉ Samuel L. Zelinka, samuel.l.zelinka@usda.gov; Joseph E. Jakes, joseph.e.jakes@usda.gov; Grant T. Kirker, grant.kirker@usda.gov; Leandro Passarini, leandro.passarini@ccnb.ca; Christopher G. Hunt, christopher.g.hunt@usda.gov; Barry Lai, blai@aps.anl.gov; Olga Antipova, oantipova@anl.gov; Luxi Li, luxili@aps.anl.gov; Stefan Vogt, svogt@anl.gov | [1]US Forest Service Forest Products Laboratory, Madison, USA. [2]Collège Communautaire du Nouveau-Brunswick (CCNB), Campbellton, Canada. [3]Advanced Photon Source, Argonne National Laboratory, Lemont, USA.

SN Applied Sciences (2019) 1:240 | https://doi.org/10.1007/s42452-019-0249-2

Received: 17 December 2018 / Accepted: 11 February 2019

SN Applied Sciences
A SPRINGER NATURE journal

Published online: 18 February 2019

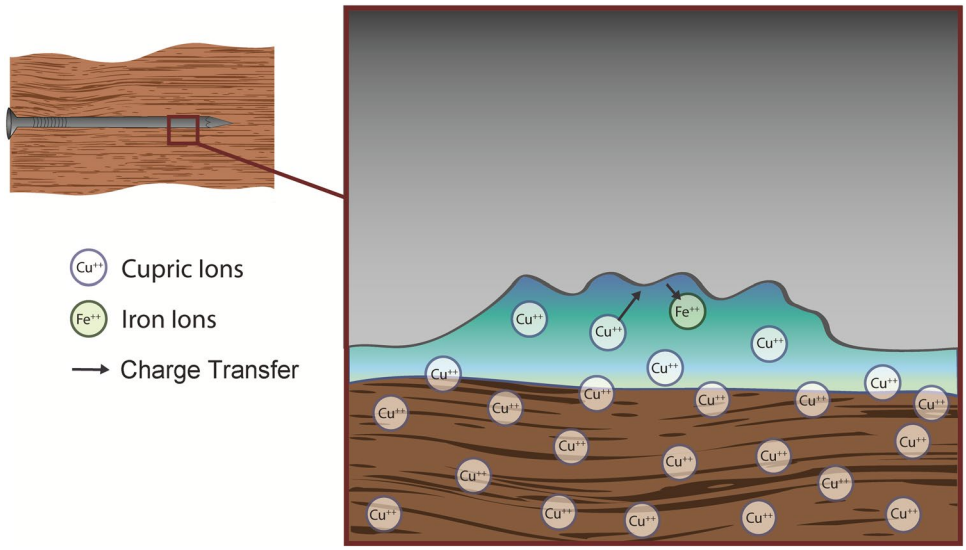

Fig. 1 Schematic illustration of the corrosion mechanism in treated wood which shows cupric ions from the wood preservative being reduced at the fastener surface. Reprinted with permission from [12]

the corrosion rate of embedded fasteners increases with increasing copper concentration in the wood, which also suggests that copper is involved in the corrosion mechanism [13]. Based on these observations, several researchers have proposed that the corrosion mechanism involves the migration of the cupric ions to the fastener surface where they are reduced as the fastener is oxidized [5, 9, 10, 12, 17].

However, despite thermodynamic and kinetic evidence that the corrosion mechanism involves the reduction of cupric ions, copper was not detected in the corrosion products, as expected, in previous studies. Zelinka et al. [18] utilized energy dispersive X-ray spectroscopy (EDS), scanning electron microscopy (SEM), and powder X-ray diffraction (XRD) to examine the corrosion products of fasteners embedded in treated wood. They found no evidence of copper in the corrosion products using these techniques. This then raised questions about whether the proposed corrosion mechanism was correct and if it was, what was happening to the reduced copper. Possible alternative hypotheses may include (1) that the copper was migrating to the fastener surface but was being reduced in the wood near the metal surface, (2) that the copper was being reduced at the fastener surface but reoxidized in a further reaction step, or (3) that the proposed mechanism was wrong entirely.

In this study, synchrotron based X-ray fluorescence microscopy (XFM) and X-ray absorption near edge spectroscopy (XANES) are employed to better understand the corrosion mechanism of metal fasteners in treated wood. XFM has been used to map out the distribution of ions in wood cell walls down to trace levels with a resolution of approximately 400–600 nm [19–23], while XANES facilitates the determination of the oxidation state of the metal ions with a similar spatial resolution to XFM. Preliminary studies have shown the possibility of visualizing copper from wood treatments in cell walls as well as determine the oxidation state of copper ions within the cell walls [24, 25]. This present study investigates the distribution and oxidation states of copper ions near the wood-metal interface for wood exposed to steel and hot-dip galvanized steel fasteners and put the findings in context of the broader understanding of corrosion of metals in treated wood.

2 Materials and methods

2.1 Sample preparation

The samples examined came from previous corrosion tests examining the corrosion of metals embedded in treated southern pine (*Pinus* spp.) [17, 18]. In these experiments, steel and hot-dip galvanized steel fasteners were driven into southern pine and exposed for 1 year at 27 °C (80 °F) close to saturation pressure by placing the wood-metal assemblies over a reservoir of liquid water. The composition of the hot dip galvanized steel coating was found to be over 95 wt% zinc [18]. After the tests were completed, the wood was split using the fasteners as a fulcrum; this allowed the fasteners to be removed from the wood without damaging the corrosion products. The wood was stored under dry (< 50% RH) conditions and the corrosion products were stored in sealed glass vials for several years until they could be examined with XFM.

Four different copper based wood preservatives were examined: chromated copper arsenate (CCA), alkaline copper quaternary (ACQ-D), copper azole (CA-C), and micronized copper quaternary (MCQ). The compositions of the preservatives and their retention in the wood are given in Table 1. The corrosion rates are also included in the table. The corrosion rates ranged from 9 to 32 μm year^{-1}.

It was shown that the differences in corrosion rates could be explained entirely by differences in the pH and copper concentrations of the various preservatives [12].

To examine the wood using XFM and XANES, the samples were cut into 2 µm thick sections. This was accomplished by first taking the blocks of wood that had been in contact with the fastener and then cutting them into small cubes. These cubes were then placed into a Leica EM UC7 ultramicrotome (Wetzlar, Germany) fitted with a diamond knife and cross sections (transverse sections) were cut dry at room temperature. The sections were then held between two 200 nm–thick low stress Norcada (Edmonton, AB, Canada) silicon nitride windows for the experiments.

The corrosion products were also examined with XFM. These corrosion products were obtained from brushing the surface of the fastener after the corrosion experiment and collecting the debris that was removed in this process. This powder was then spread onto Kapton™ tape (DuPont, Wilmington, DE) and the corrosion products were imaged on the tape.

2.2 Testing methods

XFM was performed at beamline 2-ID-E at the Advanced Photon Source at Argonne National Laboratory with a beam energy of 10.15 keV and a focused beam diameter of 0.6 µm (FWHM). Elemental maps of the wood cell walls were built in 0.5 µm step sizes and a 5 ms dwell time for each step in fly scan mode. Maps of the corrosion products were taken with a beam focused to 0.6 µm diameter, 1 µm steps, and 5 ms dwell times using an aluminum filter to attenuate the beam to prevent X-ray fluorescence detector overload. Data analysis was carried out by the MAPS software package where the full spectra were fit to modified Guassian peaks, the background was iteratively calculated and subtracted, and the elemental quantification is calibrated by a standard reference (RF4-100-S1749, AXO DRESDEN GmbH, Heidenau, Germany) [26]. One section of each sample type was examined due to time limitations of XFM beamtime.

The copper XANES scans were collected at beamline 2-ID-D at the Advanced Photon Source at Argonne National Laboratory and scanned over the copper K-edge (8980 eV) from 8960 to 9040 eV with a step size of 0.5 eV and a beam spot size of 0.2 µm. The dwell time at each energy depended on the relative signal (amount of copper) and ranged from 2 to 10 s per energy step. The dwell time was chosen by the operator prior to each scan. The data were analyzed by exporting the copper fluorescence signal and the upstream ion current from the MAPS software package [26]. The data were then imported into ATHENA (version 0.9.22) where the fluorescence signal was divided by the upstream ion current to create the X-ray absorption coefficient, "µ(E)", as a function of energy [27]. The µ(E) signal was then baseline corrected in ATHENA to create the normalized µ(E) plots that are presented in the paper. XANES scans were taken in different anatomical features such as the secondary cell wall and the middle lamella. However, the curves taken in these regions showed no differences beyond noise. Therefore, individual scans were merged to form a single curve within Athena to reduce noise.

Table 1 Preservative treatments examined with their compositions, copper concentrations, and corresponding corrosion rates [18]

	Composition	Nominal retention (kg of preservative per m^3 of wood)	Actual retention (kg of preservative per m^3 of wood)[a]	Bulk copper concentration (kg of copper per m^3 of wood)	Corrosion Rate (µm $year^{-1}$)[b]
MCQ Micronized copper quaternary	66.7 wt% CuO 33.3 wt% DDAC[c]	4	5.0	2.6	13 steel 19 galv.
ACQ Alkaline copper quaternary (type D)	66.7 wt% CuO 33.3 wt% DDAC	4	2.9	1.5	17 steel 32 galv.
CA Copper azole (type C)	96.1 wt% CuO 1.95 wt% Tebuconazole 1.95 wt% Propiconazole	1	0.7	5.4	11 steel 29 galv.
CCA Chromated copper arsenate (type C)	47.5 wt% CrO_3 18.5 wt% CuO 34.0 wt% As_2O_5	4	1.6	0.2	9 steel 16 galv.

[a]Actual retention in bulk wood as determined by Inductively coupled plasma atomic emission spectroscopy (ICP-AES)

[b]Corrosion rate measured gravimetrically after exposure to 27 °C and 100% RH for 1 year [18]

[c]DDAC, didecyldimethylammonium carbonate

3 Results and discussion

Previous research had hypothesized that copper from the wood preservatives was either reduced in the cell walls near the fastener surface or migrated to the fastener surface where it was reduced. The first hypothesis was tested with XANES. Figure 2 shows the results of the XANES scans in the wood cell walls exposed to steel fasteners; Fig. 3 presents the corresponding results from the cell walls near galvanized fasteners. The subpanels represent the results from different wood treatments. The "control" data were taken from cell walls far from the fastener surface where no iron or zinc was detected in the XFM maps and the "corrosion" data were collected in cells that contained iron or zinc. While in many cases the cells in the "corrosion" zone were depleted in copper, there was enough copper signal to collect a XANES spectrum. It can be seen in Figs. 2 and 3 that in all but one case (CA, steel), the curves lie on top of each other. Importantly, the pre-edge peak (around 8982 eV) does not change in energy or amplitude, which implies that the oxidation state did not change. These figures show that for the most part, the corrosion mechanism does not involve in situ reduction of copper from the wood preservative in the wood cell walls.

XFM gives information about the spatial location of copper, iron, and zinc in the wood cell walls near the fastener surface. Figure 4 presents XFM maps collected in wood sections cut near the interface with steel fasteners. Three different XFM maps are presented for each wood preservative: copper, iron, and a composite image where the copper and iron maps are plotted on top of each other with different colors (copper = red, iron = blue). The white chevron in the image indicates the approximate location of the fastener with respect to the wood section. The iron corrosion products can be seen in the cell walls of all four wood treatments, however, the depth to which the iron diffused varied across the treatments.

A range of behaviors can be observed across the different wood preservatives. The interaction of iron and copper is easiest to observe from the composite image. For example, the MCQ sample has red, purple, and blue regions. The cells in the red region show the copper in the cell walls from the preservative treatment. In the purple region, these cells still have most or all of the copper from the wood preservative, but iron from the fastener had diffused in as well. Finally, in the blue region, these cell walls are depleted in copper so only the iron signal is visible. While in the MCQ sample, all three regions are all visible, in the ACQ sample, however, the iron only appears in parts of the cell walls (less than 5 µm from the edge). The majority of this iron rich region also contains copper but there is a small zone on the very edge of the cells that is depleted in copper. For the CA treatment, there is a large copper depleted and iron rich region; there does not appear to be an appreciable overlap between the iron and copper rich regions. For the CCA sample, there

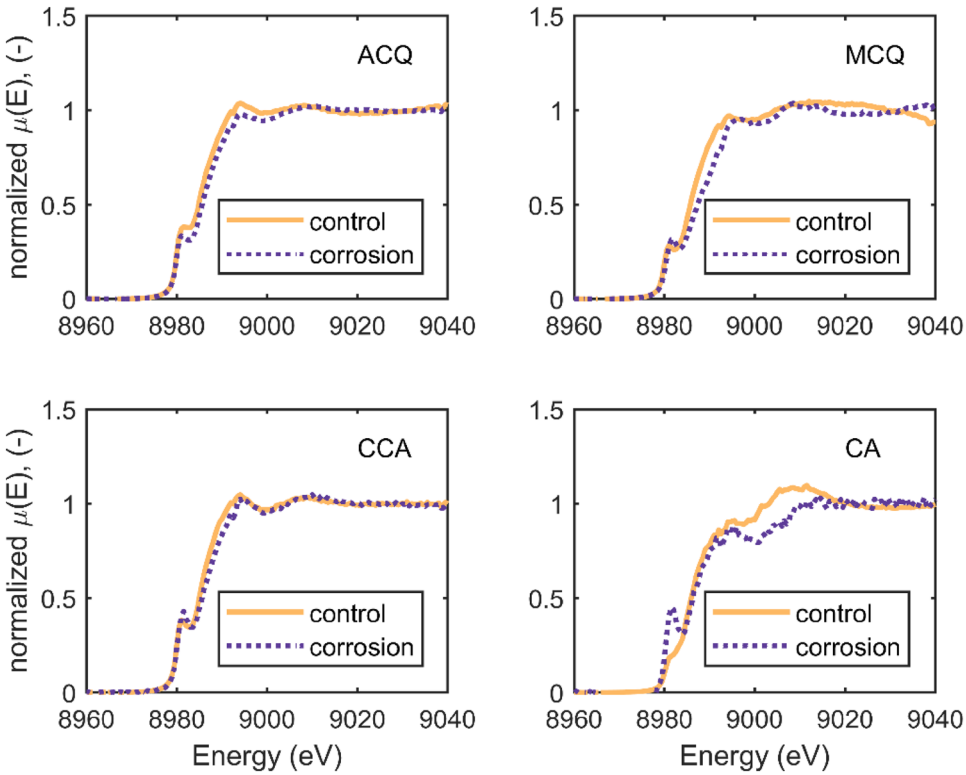

Fig. 2 XANES spectra collected in the wood cell walls adjacent to the steel fasteners

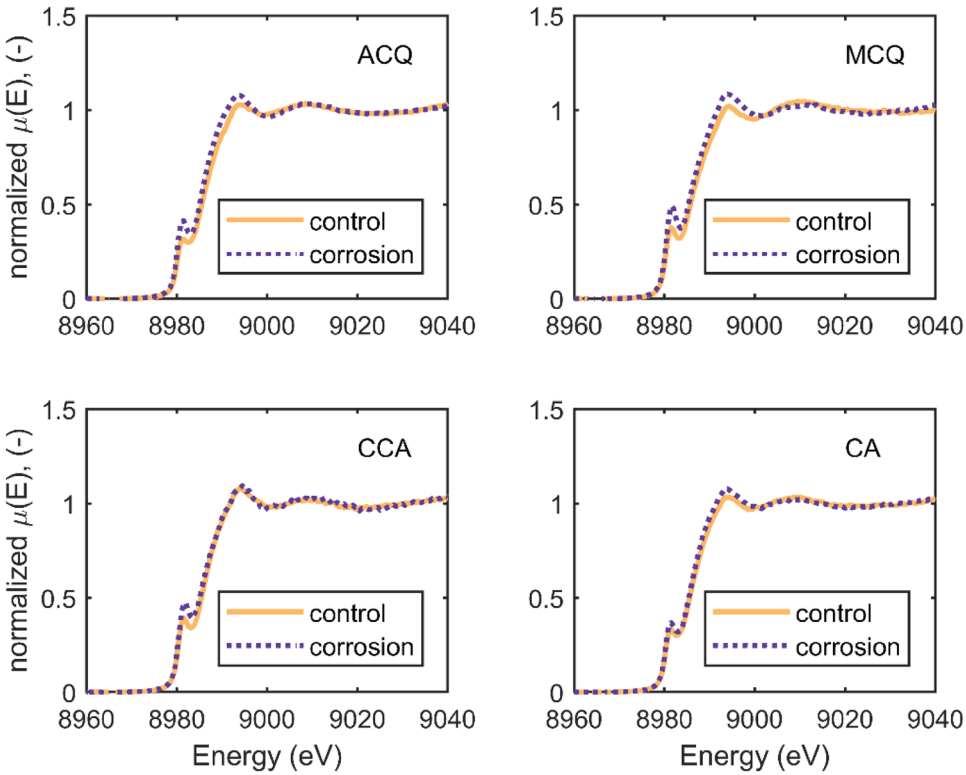

Fig. 3 XANES spectra collected in the wood cell walls adjacent to the galvanized fasteners

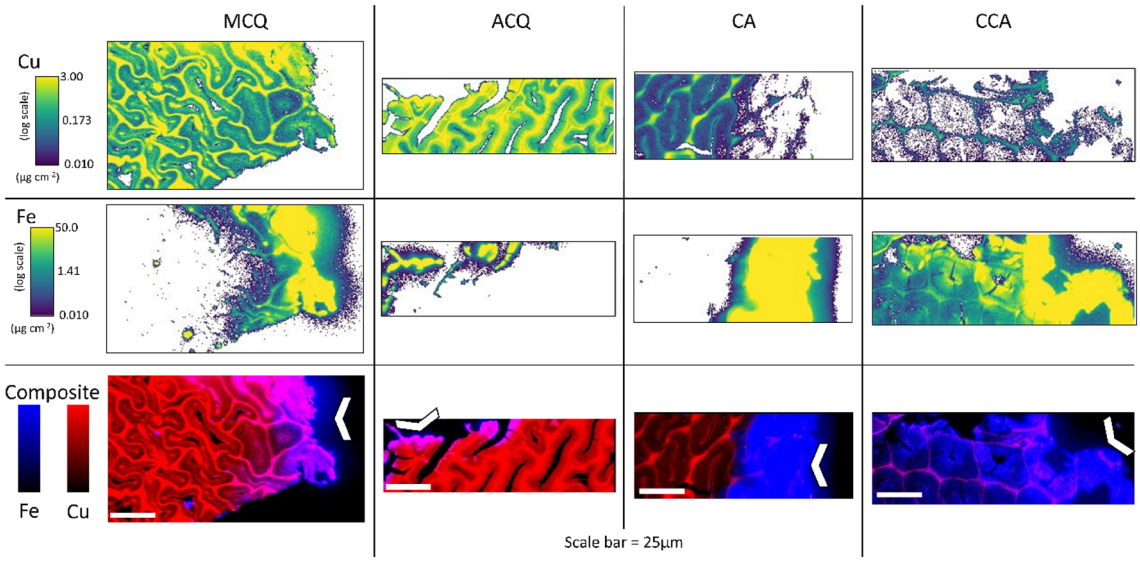

Fig. 4 XFM maps of the wood cell walls near the fastener surface of steel fasteners in 4 different treatments. The top map shows the distribution of copper and the middle map shows the concentration of iron. The bottom map shows a composite image where the copper distribution is shown in red and the iron distribution in blue; the intensity of each color is proportional to its concentration. Chevron denotes location of the fastener during exposure

is iron throughout the sample, although there is an even higher concentration of iron in the upper right corner of the image. At the same time, the entire section has less copper than the other treatments shown, likely because the CCA treatment uses less copper than the other wood preservative systems examined [3, 14]. The high amount of iron uniformly distributed throughout the sample may be a result of trace impurities in the industrial grade treatment chemicals. In previous work using XFM, cell walls of copper treated wood were found to be uniformly higher in

iron and this was attributed to impurities in the treatment [28]. Regardless of the reason for the high iron concentration, the differences in the relative amounts of iron and copper make it difficult to directly compare this image to the other wood preservative treatments. However, when examining the region closest to the chevron, it appears that there are regions of cell wall material that only contain iron and are copper depleted, similar to the other wood preservative systems.

Figure 5 is an analogous figure containing XFM maps taken from cell wall material directly adjacent to galvanized steel fasteners. Similar to Fig. 4, the top image shows the distribution of copper within the cell wall, the middle image shows the zinc concentration and the composite image on the bottom is an overlay of the two previous maps with copper in red and zinc in blue. Although the sections in Fig. 5 came from different blocks of wood that were surrounding different fasteners from Fig. 4, it is instructive to make comparisons across how the various metal fasteners performed. It appears for all treatments, there is a higher concentration of zinc in the cell walls and that the zinc has diffused farther into the cell walls when compared to the steel fasteners in Fig. 4. This should not be surprising as the measured corrosion rates of the zinc galvanized fasteners were higher than those of the steel fasteners [18]. The MCQ and ACQ samples exhibit similar behavior to that shown in Fig. 4. For MCQ there is a region of zinc with no copper at the edge closest to the fastener with a zone where both copper and zinc are present behind this edge. The ACQ sample shows very little diffusion of the corrosion products into the wood cell wall and almost no visible regions of the cell wall where only zinc is present by itself. Given that the ACQ sample had the highest corrosion rate, one would expect this sample to have a very high penetration of zinc into the cell wall and a high depletion of copper. It may be that the cells closest to where the fastener touched the wood were damaged or removed during sample preparation. The CA composite image in Fig. 5 has a large purple region where both zinc and copper are present, unlike the case for the steel fastener, there does not appear to be a large region of depleted copper. Finally for the CCA specimen, there are cells that have zinc but not copper near the fastener edge; the remainder of the sample has a very high concentration of zinc and a low concentration of copper.

While Figs. 4 and 5 are helpful in visualizing the interplay between the corrosion products in the wood cell wall and the copper concentration from the preservative in the corrosion affected zone, they have several limitations. Firstly, the sections were cut from the wood near the fastener after a corrosion test after the fasteners had been removed. While every effort was made to preserve the wood surface directly adjacent to the fastener, some cells may have been removed during fastener extraction or sectioning of the wood for the microscopy. Because of this, it is impossible to say how far any given image was from the fastener surface and whether differences in copper concentration between treatments represent a quantitative difference between the treatments or whether it was related to from where the sections were cut. These sample preparation issues are in part caused by the fact that the

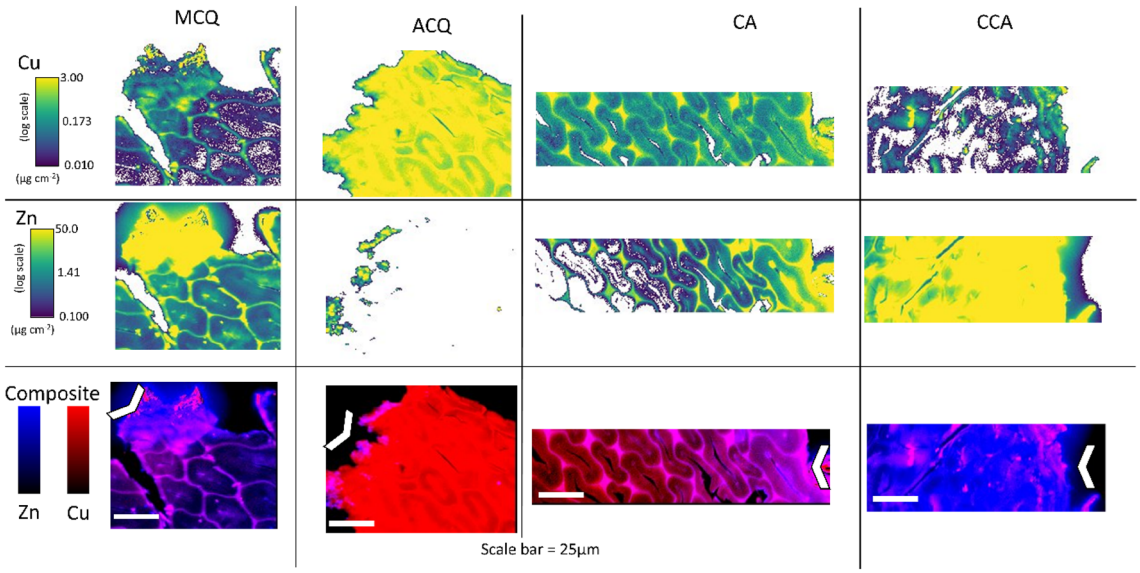

Fig. 5 XFM maps of the wood cell walls near the fastener surface of hot dip galvanized steel fasteners in 4 different treatments. The top map shows the distribution of copper and the middle map shows the concentration of zinc. The bottom map shows a composite image where the copper distribution is shown in red and the iron distribution in blue; the intensity of each color is proportional to its concentration. Chevron denotes location of the fastener during exposure

study examined samples from a long term corrosion test using real fasteners. More quantitative results may be possible in a future study by placing prepared wood samples in contact with metal. Furthermore, because of beamline constraints, only one sample could be examined for each condition. Therefore, it is unclear if the observations can be generalized to the wood preservative treatment, or represent only one position along the length of the fastener.

Even with these limitations, Figs. 4 and 5 give an idea of the range of copper and iron interactions that are happening near the fastener surface. In all cases, iron and zinc corrosion products diffused into the wood cell walls. The range of diffusion distances ranged from as small as approximately 10 µm for ACQ treated wood, to over 100 µm in CCA treated wood. Furthermore, in nearly every case, there was a region near the fastener surface that was depleted in copper and these cells were only visible in the XFM maps of iron or zinc. The depth of this copper depleted zone again had a range of observed behaviors from less than or equal to 1 µm in ACQ treated wood to as much as 50 µm for CA treated wood.

The XFM maps in Figs. 4 and 5 are some of the first experimental evidence that test hypothesized mechanism for corrosion in treated wood; namely that the corrosion mechanism involves migration and reduction of copper in the wood preservatives (Fig. 1). From these data it appears that copper from the cell walls immediately adjacent to the fastener has been depleted. It follows that copper should indeed be present in the corrosion products as there is a zone near the fastener surface depleted in copper. Previous measurements on the corrosion products using EDS and powder X-ray diffraction did not detect any copper in the corrosion products [18]. However, from Figs. 4 and 5, the total amount of reduced copper can be estimated and the amount of reduced copper would be too small to measure with those techniques. For example, the CA sample next to the steel fastener had one of the largest zones of copper depletion, 50 µm and the copper in this region was decreased from 0.26 to 0.05 µg cm^{-2}. Assuming that this section was taken directly from the edge of the fastener (radius 1.5 mm) the amount of copper in the corrosion products would be approximately 1 ng per 2 µm of fastener length, which equates to 32 µg for the entire length of the 64 mm fastener [25]. This small amount of copper would likely be undetectable with EDS with a minimum level of detection of 0.1–1 wt% [29] or powder XRD whose minimum level of detection is approximate 5 wt% [30].

An attempt was made to see if XFM could detect copper in the corrosion products. The same corrosion products analyzed with EDS and powder XRD were analyzed at the same beamline used to collect the elemental maps shown in Fig. 6 for steel corrosion products and Fig. 7 for the

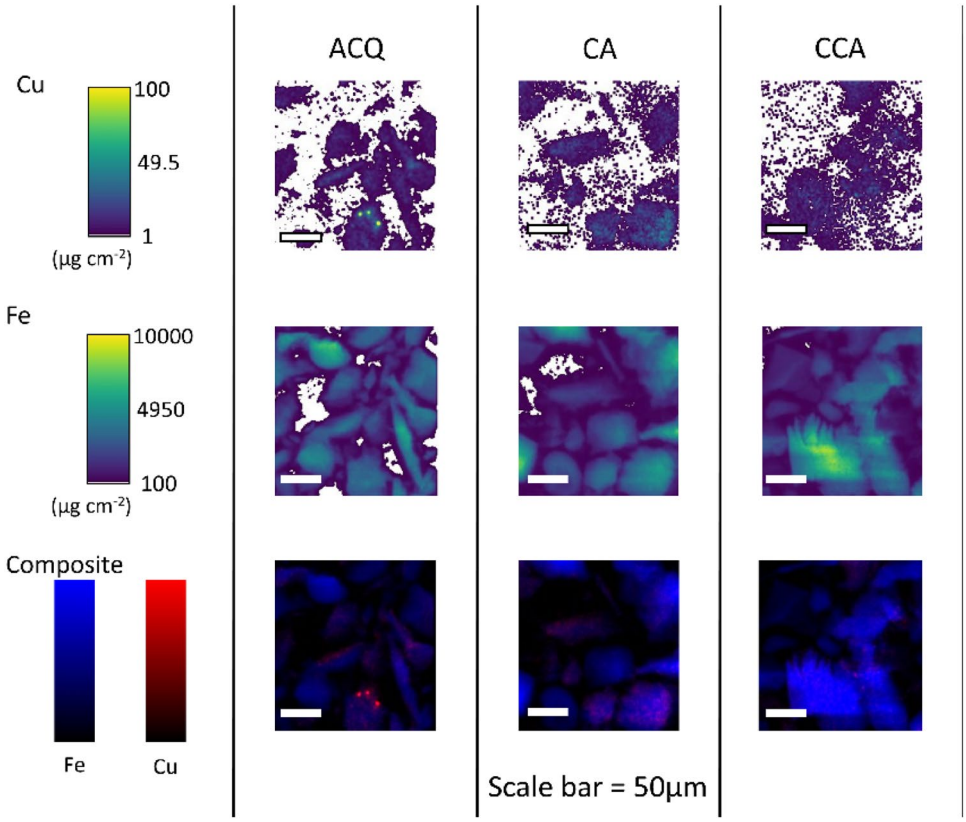

Fig. 6 XFM maps of the corrosion products collected from the surface of steel fasteners embedded in treated wood; the different wood treatments are shown in adjacent columns. The distribution of copper is shown on the top row, iron on the second, and the third row presents a composite image where the both the iron and copper distribution are shown as different colors

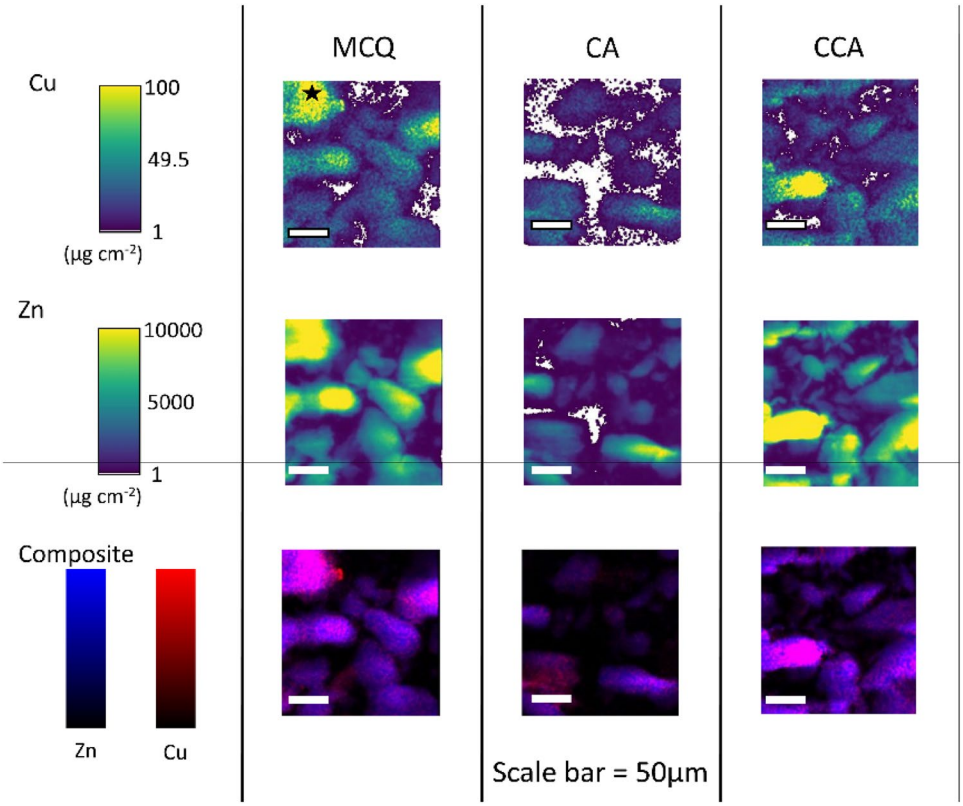

Fig. 7 XFM maps of the corrosion products collected from the surface of hot dip galvanized steel fasteners embedded in treated wood; the different wood treatments are shown in adjacent columns. The distribution of copper is shown on the top row, zinc on the second, and the third row presents a composite image where the both the zinc and copper distribution are shown as different colors

galvanized steel corrosion products. In Fig. 6 the corrosion product particles can be seen in the iron map. The copper map, also shows conglomerations of copper. However, the copper appears in much lower quantities than iron in these maps; the scale is set to 1/1000th that of iron. The composite image in Fig. 6 is important for confirming that the copper is

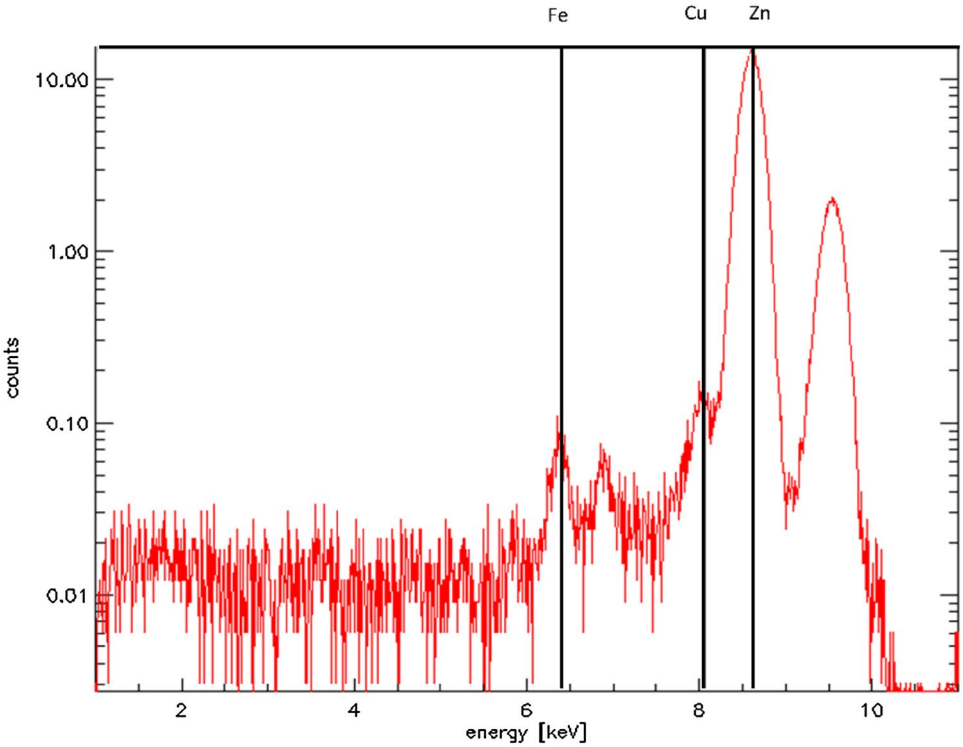

Fig. 8 XRF spectra in the region of interest denoted by a star in Fig. 7. The K_α peaks of Fe, Cu, and Zn, are highlighted by solid lines. Note that the Cu K_α peak is distinct from that of Zn

co-located within the steel corrosion products and not separate particles or random noise. In the composite images, the regions of highest copper concentration can be observed as red/purple dots within the iron particles. This suggest that coper is indeed in the corrosion products, although in very small concentrations. This is consistent both with the proposed mechanism of corrosion that involves copper reduction and with the previous measurements where copper was not detected in the corrosion products, since the concentration is so low.

Figure 7 shows the corrosion products from the galvanized fasteners; again, the shape of the particles can be easily seen from the zinc maps. In Fig. 7, the particles of corrosion products can most clearly be seen in the maps of zinc. Similar to Fig. 6, the scale for the map of copper is 1000 times smaller than that of the zinc concentration. However, in general, there appears to be more copper in the zinc corrosion products (Fig. 7) than in the steel corrosion products (Fig. 6). This can also be seen in the combined images in Fig. 7 where the corrosion products appear as purple objects, meaning that the copper is distributed throughout the zinc particles in the corrosion products.

Because the Kα peaks of copper (8.04 keV) and zinc (8.63 keV) are close, we further examined the spectra to make sure that the observed copper signal in the maps were indeed from copper and not from a wide zinc peak. The XFM spectra was examined in a region of interest with high copper concentration on the corrosion products collected from fasteners that had been in contact with MCQ treated wood. The region of interest is denoted with a star in Fig. 7. The corresponding spectra is presented in Fig. 8. In Fig. 8 the copper Kα peak can be found and is distinct from the zinc peak. We therefore conclude that there is indeed copper in the corrosion products of both steel and galvanized steel fasteners exposed to treated wood.

4 Conclusions

The copper distribution and oxidation states in the cell wall were examined using synchrotron based XANES and XFM to better understand the corrosion mechanisms of fasteners in treated wood. Further analysis of the corrosion products using XFM was performed. The major findings were:

1. In almost all cases, the copper oxidation state in the cell walls near the corrosion surface does not change.
2. Wood cell walls closest to the fastener surface are depleted in copper. Furthermore, iron and zinc corrosion products are able to diffuse into the cell walls.
3. Based off of the examination of the cell walls, the expected amount of copper in the corrosion products is below the level of detection of commonly used tools to examine corrosion products.
4. XFM images of the corrosion products confirm the presence of small amounts of copper in the corrosion products collected from steel and galvanized steel fasteners embedded in treated wood.

These observations confirm that the cathodic corrosion reaction involves the reduction of cupric ions in the wood preservatives. Furthermore, from the XANES measurements, it can be concluded that the reduction is taking place at the fastener surface rather than in situ reduction of the cupric ions within the cell walls.

Acknowledgements The use of Advanced Photon Source facilities was supported by the US Department of Energy, Basic Energy Sciences, Office of Science, under Contract Number W-31-109-Eng-38.

Funding This study was funded by the USDA Forest Service, Forest Products Laboratory. The use of Advanced Photon Source facilities was supported by the US Department of Energy, Basic Energy Sciences, Office of Science, under Contract Number W-31-109-Eng-38. This article was written and prepared by US Government employees on official time, and it is therefore in the public domain and not subject to copyright.

Compliance with ethical standards

Conflict of interest The authors declare that they have no conflict of interest.

References

1. Burkholder M (2004) CCA, NFBA, and the post-frame building industry. Frame Build News 16(5):6–12
2. Rush FA (2015) Deck collapse-4403 ocean drive. Town of Emerald Isle, Emerald Isle, NC
3. Lebow S (2004) Alternatives to chromated copper arsenate for residential construction. Res. Pap. FPL-RP-618. U.S.D.A. Forest Service, Forest Products Laboratory, Madison, WI
4. Lebow S (2010) Wood preservation. In: Ross RJ (ed) Wood handbook—wood as an engineering material. U.S. Department of Agriculture, Forest Service, Forest Products Laboratory, Madison, WI, p 508
5. Baker AJ (1988) Corrosion of metals in preservative-treated wood. In: Hamel M (ed) Wood protection techniques and the use of treated wood in construction. Forest Products Society, Madison, pp 99–101
6. Baker AJ (1992) Corrosion of nails in CCA- and ACA-treated wood in two environments. For Prod J 42(9):39–41
7. Cross JN (1990) Evaluation of metal fastener performance in CCA treated timber. In: Baker JM (ed) Durability of building materials and components. E & FN Spon, London
8. Zelinka SL, Rammer DR (2005) Review of test methods used to determine the corrosion rate of metals in contact with treated

wood. Gen. Tech. Rp. FPL-GTR-156. U.S. Department of Agriculture, Forest Service, Forest Products Laboratory
9. Kear G, Wú HZ, Jones MS (2008) Corrosion of ferrous- and zinc-based materials in CCA, ACQ, and CuAz timber preservative solutions. Mater Struct 41(8):1405–1417
10. Kear G, Wu H-Z, Jones MS (2009) Weight loss studies of fastener materials corrosion in contact with timbers treated with copper azole and alkaline copper quaternary compounds. Corros Sci 51(2):252–262. https://doi.org/10.1016/j.corsci.2008.11.012
11. Zelinka SL, Rammer DR (2009) Corrosion rates of fasteners in treated wood exposed to 100% relative humidity. ASCE J Mater Civ Eng 21(12):758–763
12. Zelinka SL, Stone DS (2011) Corrosion of metals in wood: comparing the results of a rapid test method with long-term exposure tests across six wood treatments. Corros Sci 53(5):1708–1714. https://doi.org/10.1016/j.corsci.2011.01.039
13. Zelinka SL, Rammer DR (2011) Synthesis of published and unpublished corrosion data from long term tests of fasteners embedded in wood: calculation of corrosion rates and the effect of corrosion on lateral joint strength. Paper presented at the CORROSION 2011, Houston, TX
14. Zelinka SL (2014) Chapter 23. corrosion of metals in wood products. In: Aliofkhazraei M (ed) Developments in corrosion protection. InTech, Rijeka, pp 568–592
15. Xue W, Ruddick JN, Kennepohl P (2016) Solubilisation and chemical fixation of copper (II) in micronized copper treated wood. Dalton Trans 45:3679–3686
16. Zelinka SL, Passarini L (2018) Corrosion of metal fasteners embedded in acetylated and untreated wood at different moisture contents. Wood Mater Sci Eng. https://doi.org/10.1080/17480272.2018.1544171
17. Zelinka SL (2009) Mechanism of corrosion in treated wood. University of Wisconsin, Madison
18. Zelinka SL, Sichel RJ, Stone DS (2010) Exposure testing of fasteners in preservative treated wood: gravimetric corrosion rates and corrosion product analyses. Corros Sci 52(12):3943–3948
19. Paunesku T, Vogt S, Maser J, Lai B, Woloschak G (2006) X-ray fluorescence microprobe imaging in biology and medicine. J Cell Biochem 99(6):1489–1502. https://doi.org/10.1002/jcb.21047
20. Jakes JE, Gleber S-C, Vogt S, Hunt CG, Yelle DJ, Grigsby W, Frihart CR (2013) New syncrotron-based technique to map adhesive infiltration in wood cell walls. In: Proceedings of the 36th annual meeting of the Adhesion Society, Datona Beach, FL, March 3–6, 2013
21. Zelinka SL, Gleber S-C, Vogt S, Rodríguez López Gabriela M, Jakes Joseph E (2015) Threshold for ion movements in wood cell walls below fiber saturation observed by X-ray fluorescence microscopy (XFM). Holzforschung 69(4):441–448. https://doi.org/10.1515/hf-2014-0138
22. Kirker G, Zelinka S, Gleber S-C, Vine D, Finney L, Chen S, Hong YP, Uyarte O, Vogt S, Jellison J, Goodell B, Jakes JE (2017) Synchrotron-based X-ray fluorescence microscopy enables multiscale spatial visualization of ions involved in fungal lignocellulose deconstruction. Sci Rep 7:41798. https://doi.org/10.1038/srep41798
23. Hunt CG, Zelinka SL, Frihart CR, Lorenz L, Yelle D, Gleber S-C, Vogt S, Jakes JE (2018) Acetylation increases relative humidity threshold for ion transport in wood cell walls–a means to understanding decay resistance. Int Biodeterior Biodegrad 133(1):230–237. https://doi.org/10.1016/j.ibiod.2018.06.014
24. Zelinka SL, Kirker GT, Jakes JE, Passarini L, Lai B (2016) Distribution and oxidation state of copper in the cell walls of treated wood examined by synchrotron based XANES and XFM. In: Proceedings of the 112th annual meeting of the American Wood Protection Association San Juan, PR, 2016. American Wood Protection Association, pp 172–178
25. Zelinka SL, Jakes JE, Kirker GT, Passarini L, Lai B (2016) Corrosion of metals in treated wood examined by synchrotron based XANES and XFM. Paper No. 7038. Paper presented at the CORROSION 2016, Vancouver BC, March 6–10, 2016
26. Vogt S (2003) MAPS: a set of software tools for analysis and visualization of 3D X-ray fluorescence data sets. J Phys IV 104:635–638
27. Ravel B, Newville M (2005) ATHENA, ARTEMIS, HEPHAESTUS: data analysis for X-ray absorption spectroscopy using IFEFFIT. J Synchrotron Radiat 12(4):537–541
28. Zelinka SL, Jakes JE, Tang J, Ohno KM, Bishell AB, Finney L, Maxey ER, Vogt S, Kirker GT (2018) Fungal-copper interactions in wood examined with large field of view synchrotron based X-ray fluorescence microscopy. Wood Mater Sci Eng. https://doi.org/10.1080/17480272.2018.1458049
29. Falcone R, Sommariva G, Verità M (2006) WDXRF, EPMA and SEM/EDX quantitative chemical analyses of small glass samples. Microchim Acta 155(1–2):137–140. https://doi.org/10.1007/s00604-006-0531-z
30. Williams TJ (2007) A needle in the X-ray haystack: detection limits in powder X-ray diffraction of geolocial materials. In: 2007 GSA denver annual meeting

Publisher's Note Springer Nature remains neutral with regard to jurisdictional claims in published maps and institutional affiliations.